NOT ONLY THE STRONG SURVIVE:
WEAK INTERACTIONS IN PERIPHERAL MEMBRANE BINDING PROTEINS

A THESIS
SUBMITTED TO THE FACULTY OF THE GRADUATE SCHOOL
OF THE UNIVERSITY OF MINNESOTA
BY

Jacob W. Gauer

IN PARTIAL FULFILLMENT OF THE REQUIREMENTS
FOR THE DEGREE OF
MASTER OF SCIENCE

Dr. Anne Hinderliter

August, 2011

Acknowledgements

Overwhelming thanks is owed to Dr. Anne Hinderliter, without whom none of this research would be possible. After three and a half years of (often intense) motivation, this work was finally able to come to fruition. I also thank Kristofer J. Knutson and Jesse R. Murphy who completed much of the protein purification and isothermal titration calorimetry experiments. Furthermore, I would like to thank Dr. Paulo Almeida, Dr. John Evans, Dr. Gregory Gillispie, Dr. George Makhatadze, and Dr. R. Bryan Sutton, experts in their prospective fields, for crucial advice while developing these projects.

Financial support for this work was provided by the National Institute of Health (GM064443) National Science Foundation (NSF Career – MCB 0747339), and the Montana Board of Research and Commercialization Technology (Grant 10-75).

Table of Contents

List of Tables

List of Figures

List of Abbreviations

Anx-a5 – annexin a5

Ca^{2+} – calcium ion

DSC – differential scanning calorimetry

EDTA – ethylenediaminetetraacetic acid

EGTA – ethyleneglycoltetraacetic acid

FLT – fluorescence lifetime spectroscopy

GST – glutathione-S-transferase

HEPES – 4-(2-hydroxyethyl)-1-piperazineethanesulfonic acid

ITC – isothermal titration calorimetry

KCl – potassium chloride

LUV – large unilamellar vesicle

MOPS – 3-(N-mopholino)propanesulfonic acid

MWC – Monod-Wyman-Changeux

POPC – 1-palmitoyl-2-oleoyl-sn-glycero-3-phosphocholine

POPS – 1-palmitoyl-2-oleoyl-sn-glycero-3-phospho-L-serine

SDS-PAGE – sodium dodecyl sulfate polyacrylamide gel electrophoresis

SNARE – N-ethylmaleimide sensitive factor attachment protein receptor

Syt I – synaptotagmin I

Tb^{3+} - terbium ion

CHAPTER 1: WEAK ENERGETICS AT THE MEMBRANE

Section 1.1: The Membrane

At first glance, the membrane serves only as a semi-permeable selective barrier – specifically separating distinct cellular processes from both the outside of the cell as well as from each other. However, this does not entirely describe the role of the membrane, as it is involved in a variety of cellular processes ranging from energy production to signaling [1]. To gain a better understanding of how the membrane is able to participate in these diverse functions, it is necessary to first characterize the structure, composition, and organization of the membrane.

Biological membranes are complex mixtures of lipids and proteins that arrange themselves in a manner that minimizes their associated energies. Classically, the "fluid mosaic model" was used to describe this arrangement [2]. This model accurately depicted the arrangement of phospholipid molecules into a bilayer as the optimal means to avoid interactions between the hydrophobic acyl chains of phospholipids and water, and also captured the integration of certain proteins within the membrane as a mechanism to sequester their hydrophobic regions from water. This model further predicted that hydrophobic and hydrophilic interactions would be the predominant forces, suggesting that the individual lipids and proteins within the membrane would mix within the membrane essentially randomly.

Since this model was proposed, however, deviations have been observed. Regions of the membrane enriched in certain types of lipids (lipid domains or lipid 'rafts') have been identified [3]. Integral membrane proteins involved in certain signaling pathways are

known to co-localize on the membrane [4]. Clearly, then, the assumption of random mixing is insufficient to describe the organization of the components within the membrane. These key deviations from the “fluid mosaic model” can be explained by considering interactions between the membrane components. The assumption of random mixing precludes any significant interaction between the individual membrane components having a contribution to the overall membrane structure. Recently, however, it has been shown that interactions between individual lipid molecules [5], individual proteins [4], or even between lipids and proteins [6] were all able to rearrange the organization of lipids and proteins at the membrane surface.

What is the commonality between these interactions? In general, the magnitudes of these interactions are small – on the order of a 0.1 to 10 kcal/mol. (For reference, the energy associated with hydrolysis of ATP into ADP and inorganic phosphate releases approximately 7.3 kcal/mol [1].) Exploitation of weak interactions may seem counterintuitive; when considering accomplishing some physiological goal such as folding a protein or triggering a signaling cascade, it seems as though highly stable, highly selective interactions would be advantageous. However, in a biological context, most processes need to be reversible. (For instance, consider cellular signaling, where turning the message “off” is as crucial as turning it “on”.) In essence, strong interactions do not allow what is done to be easily undone, making this option impractical in biology. Furthermore, weak energetics imply a certain degree of flexibility, allowing fewer proteins to be necessary for achieving a wider range of physiological responses.

Section 1.2: Peripheral Membrane Proteins: Annexins and C2 Domains

One class of proteins, known as peripheral membrane proteins, is categorized according to a weak association between the protein and membranes (fluid mosaic paper). These proteins are not integrated into the membrane (that is, they are not buried within the lipid bilayer); rather, they associate with the surface of the membrane. In this thesis, two common examples of these proteins, the annexins and the C2 domains, are discussed.

Several commonalities exist between these two proteins. Both the annexins and the C2 domains are able to weakly associate with lipid membranes, and they both show preference for membranes containing negatively charged, acidic phospholipids (most notably phosphatidylserine). This preference for one lipid over another provides a means to demix lipids within the membrane. They are also known to bind calcium ion (Ca^{2+}), a common second messenger in eukaryotes, in a lipid dependent manner [7-8]. Furthermore, both are commonplace in cells – C2 domains are widespread in the human genome and are found in a wide variety of proteins (including, but not limited to Protein Kinase C [9], ferlins [10], and of most importance for this work, the synaptotagmins [11]), and while there are only a handful of annexins, they are highly expressed [12].

Despite these similarities, these two proteins are structurally quite different. Annexins consist of one domain made largely of alpha helices (Fig. 1.1, Left Panel) [12], while the C2 domains are predominantly beta sheets (Fig. 1.1, Right Panel) [11] and exist only as subunits of larger proteins. Also, the cellular functions of the various C2 domain-containing proteins are generally well established (though the mechanistic details are often still in question), while the purpose of the annexins is still a mystery. Moreover, there is a difference in the extent to which these proteins selectively associate with

acidic phospholipid over neutral phospholipids – the C2 domains are able to more specifically bind phosphatidylserine (negatively charged) lipids over phophatidylcholine (neutral) lipids as compared to the annexins [7-8].) This difference suggests a difference in their abilities to demix the membrane surface.

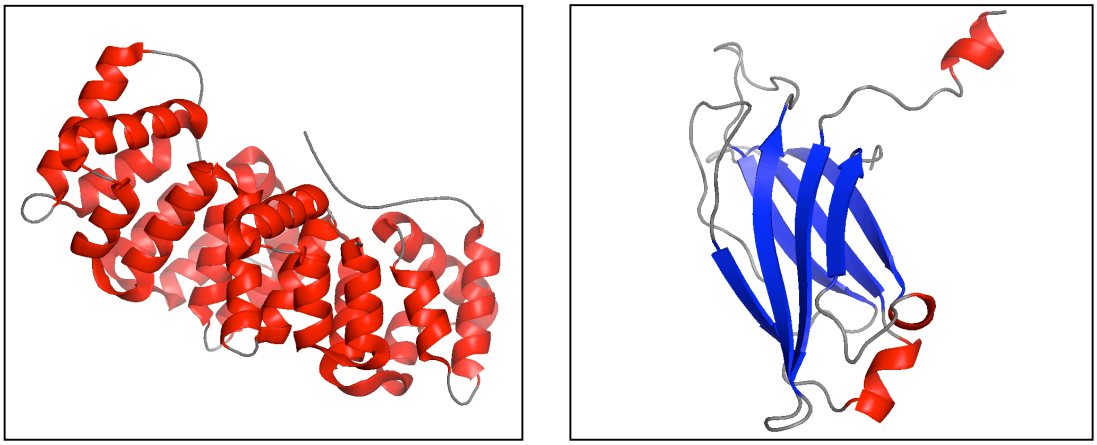

Figure 1.1: Structures of Rat Annexin a5 [13] (left) and Human Synaptotagmin I C2A [11] (right). Alpha helices are depicted in red; beta sheets are depicted in blue. PDB IDs: 2RAN (left) and 1RSY (right).

Section 1.3: Thermodynamics as a Tool

The similarities and differences between the annexins and the C2 domains provide a unique perspective to compare and contrast the effects of peripheral membrane proteins on the membrane organization in general. However, by their very nature of being weak, the associated interactions are difficult to measure. At no point do these systems exist in only one state; rather, they are continuously in dynamic equilibrium, exchanging between many states. Each state would exist with a given probability that is dependent on that state's associated free energy. This property often disallows many simplifying assumptions that could ease interpretation of the data.

One means to account for a distribution of states and the associated distribution of statistical likelihoods is through the use of partition function analysis [14]. Partition functions are a thermodynamic tool that not only more adequately describe our systems of interest, but they also have predictive power – we can predict what the distribution of states would be by extrapolating from a reference condition to a variety of others. (For example, this extrapolation could occur as a function of temperature, ligand concentration, or both.) This is a particularly useful approach when the interactions involved are weak, as measurements can be made on the overall system, and modeling can be used to deconvolute the individual states' contributions to the overall observable.

By utilizing the tool of thermodynamics in this way, both the simultaneous binding of annexin a5 (anx-a5) to its ligands (Chapter 2) as well as the thermal denaturation profile of Synaptotagmin I (Syt I) in various ligand conditions (Chapter 3) were characterized.

CHAPTER 2: WEAK MEMBRANE ASSOCIATION ENABLES COOPERATIVE BINDING OF CALCIUM ION BY ANNEXIN A5: AN ISOTHERMAL TITRATION CALORIMETRY ANALYSIS

Section 2.1: Introduction

We propose that a role of the membrane is to provide peripheral membrane-binding proteins a means to bind other ligands in a cooperative manner. Through the use of linkage relationships and a global approach to fitting a thermodynamic cycle, the impact of membrane association on Ca^{2+} binding and Ca^{2+} binding on membrane association was ascertained for annexin a5 (anx-a5). We find it is the protein state that has a weak ligation with the membrane in the absence of Ca^{2+} that enables cooperative Ca^{2+} binding.

The membrane at its simplest is a barrier. At its most fundamental, this barrier enables the compartmentalization of distinct chemical processes, a trait that is one of the primary differences between eukaryotes and prokaryotes. At its most complex, we suggest that the components of the membrane, based upon their organization, have the capacity to transduce information [5, 15]. The primary components of the biomembrane, lipids and proteins, distribute non-ideally to optimize favorable contacts and minimize free energy. Thus, the structural organization of the membrane impacts information flow into an out of the eukaryotic cell. The ability of membranes to provide a responsive surface by virtue of the weak, yet cooperative interactions between lipids allows signals to be amplified at the membrane surface by readily altering the distribution of membrane-associated

proteins [3]. In this way, lipid membranes are not simply a surface upon which proteins adhere; they are also able to sensitively modulate the affinity of protein interactions via changes in how the lipids interact with one another within the membrane [14]. Here, we bridge these concepts and find that membrane association by a protein, anx-a5, with specificity toward acidic phospholipid alters the probability of the protein to respond to a second messenger, Ca^{2+}.

Annexins, of which there are 11 forms in humans, have a variety of binding partners in addition to membrane and Ca^{2+} [16]. The annexins may be compared and contrasted with other types of membrane-associated proteins, in particular a class of binding motifs known as the 'C2' domains. The C2 domains have affinities that overlap with the membrane and Ca^{2+} affinities of the annexins [17], but they are structurally distinct. The annexins are single domain proteins largely consisting of repeating alpha helices [12], whereas the C2 domains exist solely as modules within proteins and are predominantly beta sheets [11]. Furthermore, C2 domains variants are orders of magnitude more prevalent in the human genome than the annexins, as the C2 domains are commonly found in proteins primarily involved in membrane trafficking and signal transduction [18]. To contrast, the exact function of the annexins is unknown, yet they encompass some 2% of all intracellular protein [12]. This surprising abundance of the annexins suggests a defined cellular role to merit such high expression levels. Moreover, they are an ancient family of proteins that are highly conserved throughout evolutionary history, again attesting to a primary function in the cell. One ancestral model has identified an evolutionary predecessor to the annexins where membrane association (rather than Ca^{2+} binding) was found to be the crucial property necessary for function [19]. We suggest that the annexins have not only conserved their ability to interact with

membrane, but they have also tuned this ability such that they can modulate membrane organization (that is, lipid domains) [6, 20]. We now find that it is not only the weak interactions between the lipids within the membrane surface that convey a cooperative response, but also the weak interaction between a peripheral protein and membrane that allows the protein to cooperatively bind a non-membrane ligand. Thus, our results are relevant to understanding membrane-associated proteins in general as well as contributing to defining the specific role of the annexins in cellular function.

We had previously defined the apparent cooperative interactions of anx-a5 with cation and membranes through use of a Ca^{2+}-mimic, terbium ion (Tb^{3+}) and linkage relationships [8]. An allosteric transition model fit the experimental data where the presence of acidic phospholipid increased the affinity of the protein for cation compared to solution affinity. It is the shift to higher cation affinity when the protein is membrane associated that conveys cooperativity. However, a Ca^{2+} mimic was utilized (Tb^{3+}), as annexins do not have an endogenous source of signal change to monitor ligation. If the ligation of Ca^{2+} and phospholipid was fairly strong, through the use of linkage relationships to protein denaturation, equilibrium association constants could be extracted [21]. However, annexins did not exhibit reversibility in their denaturation [22], precluding both this technique as well as evaluating a mutation such as upon introduction of a cysteine for labeling. It is also problematic to use most fluorescent probes that can fluorescently transfer energy to the endogenous tryptophan of the anx-a5 as this tryptophan is weakly fluorescent. Thus, to measure the interaction of anx-a5 using its endogenous ligands of Ca^{2+} and acidic phospholipid, isothermal titration calorimetry (ITC) was selected.

Using ITC, the magnitudes of the interactions of Ca^{2+} and phospholipid with anx-a5 were measured. A global accounting for the sources of the heat of binding was expressed in a heat partition function. We find our data with Ca^{2+} and a binary lipid mixture of acidic and neutral phospholipid is consistent with an allosteric transition model. The model implies a small population of the protein is membrane-associated in the absence of Ca^{2+}, and that upon introduction of Ca^{2+}, this membrane-associated population binds cation with greater affinity than in solution alone. This is the basis of the binding cooperativity. Furthermore, since anx-a5 exhibits greater affinity for certain lipids over others, the composition of the membrane can then poise the system at the brink of a cooperative response by tuning the membrane composition such that this weak membrane association is fostered.

Section 2.2: Materials and Methods

Subsection 2.2.1: Materials

Both 1-palmitoyl-2-oleoyl-sn-glycero-3-phosphocholine (POPC or 16:0,18:1PC) and 1-palmitoyl-2-oleoyl-sn-glycero-3-phospho-L-serine (POPS or 16:0,18:1PS) were from Avanti Polar Lipids, Inc. (Birmingham, AL). Potassium chloride (KCl) was Puriss-grade and 3-(N-morpholino)propanesulfonic acid (MOPS) was Biochemika grade from Fluka Chemical Corp. All buffers used were decalcified using Chelex-100 ion-exchange resin from Bio-Rad Labs.

Subsection 2.2.2: Purification of Rat Annexin a5

Purification of wild-type *Rattus norvegicus* anx-a5 was based on Ca^{2+}-dependent binding to membrane. cDNA encoding rat anx-a5 was kindly provided by H. Sohma (Sapporo Medical University School of Medicine) and was transformed into *Escherichia coli* Bl-21 cells. Overexpression was initiated by the addition of 1mM isopropyl-ß-D-thiogalactopyranoside at optical densities between 0.4–0.8. After 5hr induction, cells were harvested by centrifugation and lysed by sonication in 20 mM MOPS, 100 mM KCl, 10 mM calcium chloride and 1mM phenylmethanesulfonylfluoride at pH 7.5. Cellular debris was pelleted by centrifugation at 16,000 rpm for 30 min. The pellet, containing anx-a5, was then resuspended in 20 mM MOPS, 100 mM KCl, and 20 mM EDTA at pH 7.5, and gently stirred overnight to release anx-a5. The mixture was then centrifuged and sterile-filtered through a 0.45 µm filter, dialyzed against 20mM 4-(2-hydroxyethyl)-1-piperazineethanesulfonic acid (HEPES) and 5mM magnesium chloride at pH 8.0, and incubated with benzonuclease (Novagen 90% purity) at a concentration of 10 units/ml for 7 hr at 4°C. The protein solution was applied to a pre-equilibrated Q-Sepharose Fast Flow anion exchange column and eluted using a linear gradient of sodium chloride

containing 20 mM HEPES and 1 mM 2-mercaptoethanol at pH 8.0. Fractions containing anx-a5 were pooled and filtered with 0.20 µm filter. Recombinant anx-a5 was then extensively dialyzed in 20 mM MOPS, 100 mM KCl (in excess of 8 L) and passed through Chelex-100 resin to remove contaminating Ca^{2+}. Final purity of anx-a5 was >95% by SDS-PAGE densitometry. The protein was concentrated using Amicon Ultra 15 Centrifugal Filter Unit (30,000 kDa cutoff) from Millipore, and the final concentration was determined using a Nanodrop at 280 nm (21,050 $M^{-1}cm^{-1}$).

Subsection 2.2.3: Preparation of Lipid Vesicles

Large unilamellar vesicles (LUVs) composed of POPC:POPS (60:40) were prepared by Aliquotting stock solutions of lipid in chloroform into borosilicate culture tubes using gastight syringes (Hamilton Co., Reno, NV). Samples were dried to a thin film under a gentle stream of argon and dried briefly under a vacuum of less than 20 mTorr before be lyophilized from benzene/methanol (19/1, v/v). Lipids were hydrated in the dark above its gel-fluid phase transition temperature with decalcified 20 mM MOPS, 100 mM KCl, pH 7.5, under argon. LUVs were prepared by extruding a multilamellar vesicle dispersion through a sandwich of prefilters around a 0.1 µm pore size polycarbonate filter (Avanti Polar Lipids, Inc.) at least 31 times.

Subsection 2.2.4: Isothermal Titration Calorimetry (ITC)

ITC experiments to determine the binding of Ca^{2+} and various lipids to anx-a5 were performed on a TA Instruments Nano ITC at 15°C. Both the Ca^{2+} and lipid titrant solutions were prepared in the protein dialysate that was saved after concentrating the protein. This consisted of 20 mM MOPS, 100 mM KCl, pH 7.5 that was passed through Bio-Rad 100 Chelex resin to remove cation impurities and filtered using a 0.2 µm sterile

filter. The Ca^{2+} concentrations used in the experiments was verified through the use of BAPTA (Invitrogen/Molecular Probes) and Ca^{2+} electrode (Fisher). The titrant lipid concentration was verified by phosphate assay as described in Kingsley and Feigenson [23]. The anx-a5 concentration was directly measured using spectrophotometry (extinction coefficient of 21,050 $M^{-1}cm^{-1}$ at 280 nm) prior to the experiment. For all experiments, the stir speed was 250 rpm and the interval between injections was 300 s. For the Ca^{2+} titration into anx-a5 in the absence of membrane, a 9 mM Ca^{2+} solution was injected in a 1 µl injection to displace air from the syringe followed by 27 x 9 µl injections. The cell concentration of protein was 0.09 mM. Increased concentrations of protein for this particular experiment often resulted in precipitation. For experiments in which Ca^{2+} was injected in the presence of both anx-a5 and membrane, a 1.5 mM Ca^{2+} stock was added to 0.024 mM anx-a5 by a 1 µl injection to displace air from the syringe followed by 27 x 9 µl injections. The lipid concentration of 1.0 mM was the same in both the cell and the syringe so that only the enthalpy of binding between anx-a5 and Ca^{2+} in the presence of membrane could be measured. To obtain the enthalpy of binding for Ca^{2+} to anx-a5 in the presence of membrane, raw heats were integrated and the heat of dilution subtracted by injecting the Ca^{2+} and lipid into buffer containing the same concentration of lipid without protein. For lipid titration experiments, the calorimetric sample cell was filled with 1.3 ml of thoroughly degassed solution consisting of 0.029–0.100 mM anx-a5 and 0.50 mM Ca^{2+}, while the syringe was loaded with 250 µl of 30 mM total lipid (LUVs composed of a 60:40 mixture of POPC:POPS) and 0.50 mM Ca^{2+}. The use of the same Ca^{2+} concentration in both the cell and the syringe allowed only the enthalpy of membrane binding to be measured. This Ca^{2+} concentration represents 95% saturation of anx-a5 by Ca^{2+}. Lipid titrant was added in a 1 µl injection to displace air from the syringe followed by 27 x 9 µl injections. The first two data points were removed due to

subsaturation of the protein for lipid (determined using the lipid binding affinity (K_L) as derived from Eq. 2.4). For membrane titrations, raw heats were integrated and the heat of dilution subtracted by injecting the lipid and Ca^{2+} into buffer containing the same concentration of Ca^{2+} without protein.

Between experiments, the sample cell was cleaned with an aqueous solution of 15% Contrad-70, 15% methanol, followed by a methanol rinse to remove any contaminating lipids. Following solvent cleaning, exhaustive rinsing with Milli-Q water was used to clean the sample cell. Also, a buffer-buffer titration was conducted as a control ensuring that interfering heats in the buffer were not present.

Section 2.3: Results

Subsection 2.3.1: Analysis Approach

In the simplest of binding models, a protein (P) could bind *n* number of ligands (X) with equal affinity. In this system, the total protein concentration is represented as Eq. 2.1.

$$[P_T] = [P] + [PX] + [PX_2]\ldots + [PX_n] \quad (2.1)$$

Where [P] represents free protein and [PX], [PX_2], etc. represents the different forms of protein bound to ligand. The affinity of the protein for this ligand could be expressed as an equilibrium constant K = [PX]/[P][X] where [X] represents the free ligand concentration. In this model protein, all possible ligation states could be expressed as a partition function Q (Shown in Eq. 2.2).

$$Q = [P]/[P] + [PX]/[P] + [PX_2]/[P]\ldots [PX_n]/[P] = (1 + K[X])^n \quad (2.2)$$

Each of the terms in this equation (1, K[X], etc.) is a mathematical representation of the statistical likelihood of existing as a different ligation state of the protein. Furthermore, during an ITC experiment, free ligand concentration [X] is changing from injection to injection as a function of increased total ligand concentration. Thus, after each injection point, the individual terms that sum together to describe Q would change, numerically representing a redistribution of the statistical weights associated with the unique ligation states of the protein. This mathematical description of the states in which the protein can exist can be extrapolated to more complex binding models.

Assuming that ligand binding to this protein was not athermal, measurable changes in heat as a result of ligand binding could be observed in an ITC experiment [24]. This is because upon formation of each P-X interaction, there is a heat of binding (*ΔH*) that is released or absorbed. Within a given set of equivalent sites, the expected response for ligand binding to a binding site would be an equivalent *ΔH*. Throughout the titration experiment at each *i*th injection, there would exist a distribution of bound (for this example, just Ca^{2+}) and free protein that is represented by the partition function *Q*. Upon an introduction of more ligand via an additional *i+1*th injection, by Le Chatelier's principle, more of the protein would bind ligand. This would redistribute the protein states. The heat associated with this redistribution, due to this increase in the ligand bound state is what is actually measured by the calorimeter, and can be determined directly from the area under each peak as shown in the raw data (Fig. 2.1, 2.2, and 2.3; top panel).

To fit a binding model of any complexity to these data, one must use an expression that describes the difference between the total heat required to create the *ith* distribution and that required to create the *i+1* distribution in terms of known values. Unfortunately, the partition function is expressed in terms of free ligand concentration [X], a value that is not easily determined experimentally. However, what is known throughout the titration are the total concentrations of ligand and protein ($[X_T]$ and $[P_T]$, respectively) that have been added at each injection. Thus, the differential heats resulting from each injection are plotted as a function of the $[X_T]$:$[P_T]$ ratio (Fig. 2.1, 2.2, and 2.3; middle panel). The free ligand concentration [X] can be determined from the known values of $[X_T]$ and $[P_T]$ using the mass balance relationship for total ligand $[X_T] = [X]_{bound} + [X]$. The concentration of ligand that is bound, $[X]_{bound}$, can be described in terms of the bound

fraction of the total protein [P_T], accounting for the binding stoichiometry. Determination of the free ligand concentration allows the data to then be fit to various binding partition functions.

Traditionally, binding isotherms are plotted in a cumulative manner as a function of free ligand [X]. To achieve this manner of visualizing the data, the summative heats gathered throughout each experiment were plotted as a function of the increasing free ligand concentration calculated from the known and fitted values. This representation of the data is shown (Fig. 2.1, 2.2, and 2.3; bottom panel).

Subsection 2.3.2: Ca^{2+} Binding by anx-a5 in the Absence of Membrane

The titration of anx-a5 with Ca^{2+} in the absence of membrane is shown in Fig. 1. Here, the measured heat of binding was best fit using a model describing independent calcium binding sites with equal affinity. This model is the simplest of ITC models, and it is particularly convenient because it is capable of analytically describing the data in terms of known quantities (total protein concentration and total ligand concentration) and three fitted parameters. These parameters are: i) n, the number of binding sites, ii) K_0, the affinity of the binding sites, and iii) ΔH_0, the average heat released by each binding event. Fit results of this titration data using this model showed n = 5.0 ± 0.4 binding sites with affinity K_0 = (3.1 ± 0.3) x 10^3 M^{-1} ($K_{D,0}$ = (330 ± 40 μM) and heat of binding ΔH_0 = -2.4 ± 0.2 kcal/mole.

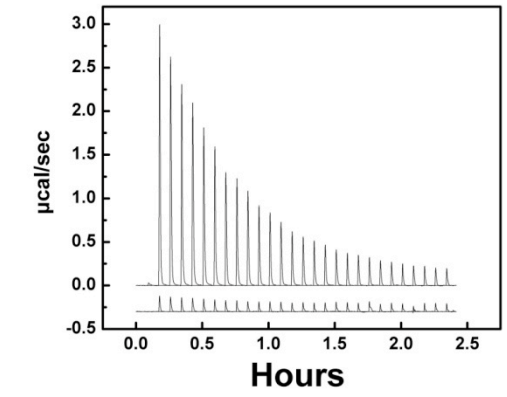

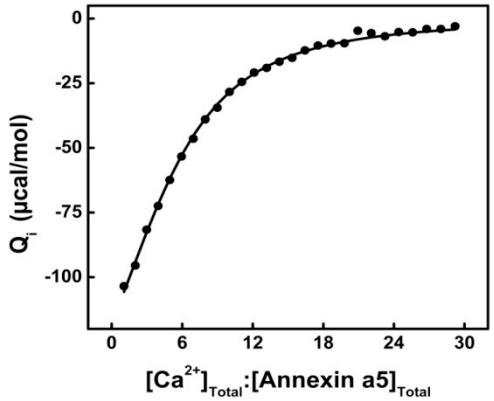

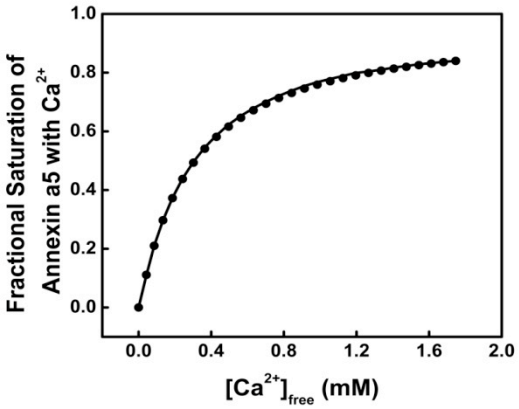

Figure 2.1: Results of the titration of 90 µM anx-a5 with Ca^{2+} at 15°C. *Top:* Raw ITC data. *Middle:* Integrated heats of binding as a function of ligand to protein ratio. *Bottom:* Binding isotherm of fractional saturation as a function of free [Ca^{2+}].

Subsection 2.3.3: Ca^{2+} Binding by anx-a5 in the Presence of Excess Membrane

The titration of anx-a5 with calcium in the presence of membrane is shown in Fig. 2.2. These data are clearly more complex than those in the absence of membrane. There are two recognizable trends in the data: an initial trend with negative slope followed by a second trend with positive slope. This complexity suggests that there are at least two heat producing processes occurring, and that the heats associated with these processes are of opposite sign. One of the limitations of ITC is that during an injection, all heats caused by any heat evolving process are added together and measured as a single, overall heat. Thus, it is difficult to distinguish the individual processes and their separate contributions to the overall heat.

To analyze these data, it was assumed that only two distinct Ca^{2+} binding processes were responsible for the two trends in the overall measured heat, the first of which was endothermic and the second of which was exothermic. Furthermore, it was assumed that the first endothermic binding sites were equivalent with high affinity, while the exothermic binding sites were equivalent with lower affinity. For simplicity, it was assumed that the total number of cation binding sites was conserved, regardless of the presence or absence of membrane. (That is, $n_{1a} + n_{1b} = n = 5$.) Deconvolution of the heat of binding produced by both sets of sites was achieved by fitting the individual contribution of each set within the data to the independent, equivalent sites model in an iterative fashion. These results suggest that there were $n_{1a} = 2.0 \pm 0.1$ sites with affinity $K_{1a} = (1.0 \pm 0.1) \times 10^5$ M^{-1} ($K_{D,1a} = 10 \pm 2$ μM) and heat of binding $\Delta H_{1a} = 4.6 \pm 0.2$ kcal/mole (the endothermic, high affinity sites) and $n_{1b} = 3.0 \pm 0.3$ sites with affinity $K_{1b} = (5.6 \pm 0.3) \times 10^3$ M^{-1} ($K_{D,1b} = 180 \pm 10$ μM) and heat of binding $\Delta H_{1b} = -13.8 \pm 1.4$ kcal/mole (the exothermic, low affinity sites).

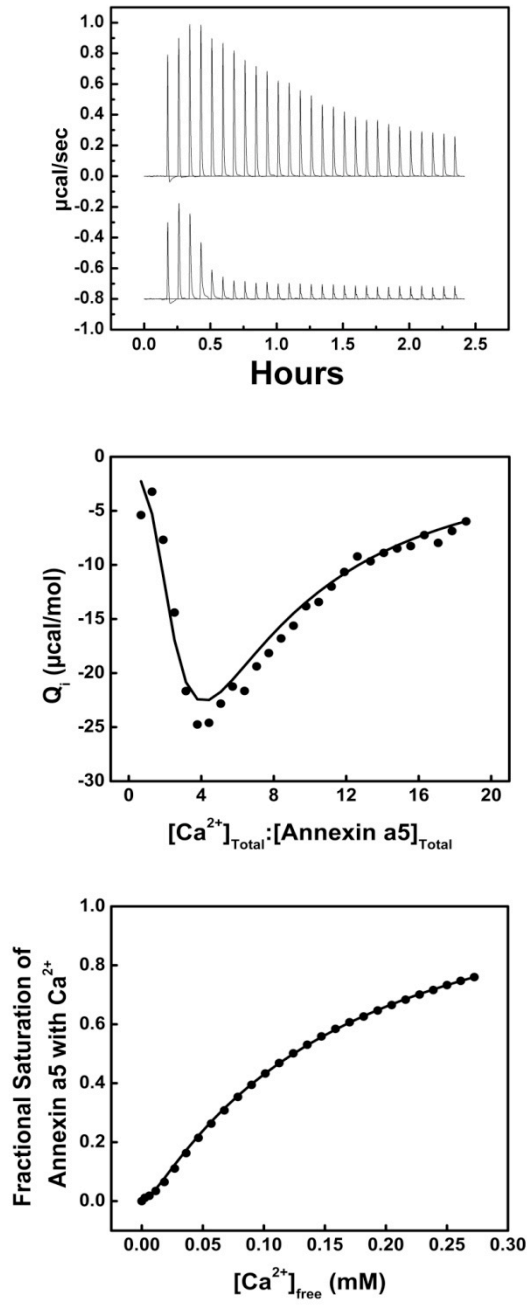

Figure 2.2: Results of the titration of 24 µM anx-a5 with Ca^{2+} in the presence of 2 mM total lipid as LUVs made of a 60:40 mixture of POPC:POPS at 18°C. *Top:* Raw ITC data. *Middle:* Integrated heats of binding as a function of ligand to protein ratio. *Bottom:* Binding isotherm of fractional saturation as a function of free [Ca^{2+}].

Subsection 2.3.4: Membrane Binding by anx-a5 in the Presence of Saturating Ca^{2+}

The titration of anx-a5 with phospholipid membranes (LUVs composed of a 60:40 mixture of POPC:POPS) in the presence of Ca^{2+} is shown in Fig. 2.3. These observations were best fit using a variation of the independent sites model that accounts for differences between binding small ligands and binding a surface. In ligand binding, it is assumed that at each binding site there exists 1:1 stoichiometry – for every site that is filled there is one ligand that is removed from solution. In the case of peripheral membrane binding proteins, however, a single binding event involves the protein occupying several lipid molecules. In the independent, equivalent sites model, this difference is becomes realized in the parameter n; it represents not only the number of binding sites per protein molecule, but also the number of ligand molecules that are no longer free as a result of the binding event. In membrane binding, these two values are different, and thus each occurrence of n within the model must be scrutinized as to exactly what it is representing.

Furthermore, it is noteworthy that this increased complexity does not increase the number of parameters used in the fits. This is because the number of binding sites per protein molecule is assumed to be 1 (that is, anx-a5 can only bind to one liposome and that liposome is a single binding site). Thus, the data can still be described using a modified form of the equivalent, independent sites model in terms of known quantities and only three parameters: i) K_{app}, the affinity of anx-a5 for the membrane in saturating Ca^{2+} conditions of 0.5mM, ii) ΔH_{app}, the heat released upon membrane binding, and iii) z, the anx-a5:lipid molecule binding stoichiometry. These results show that anx-a5 binds membrane composed of a 60:40 ratio neutral lipids to negatively charged lipids arranged as LUVs with an affinity K_{app} = (5.7 ± 0.4) x 10^4 M^{-1} ($K_{D,app}$ = 18 ± 1 μM) and heat of

binding ΔH_{app} = -19.4 ± 0.1 kcal/mole with an average binding stoichiometry of z = 69.7 ± 0.3 lipids per protein molecule. A lipid has a first ring of 6 nearest neighboring lipids, then 12 nearest neighbors, 18, 24, etc. Hence, 60-70 lipids/protein corresponds to only 4-5 layers of hexagonally packed lipids, which is consistent with the known relative size of anx-a5.

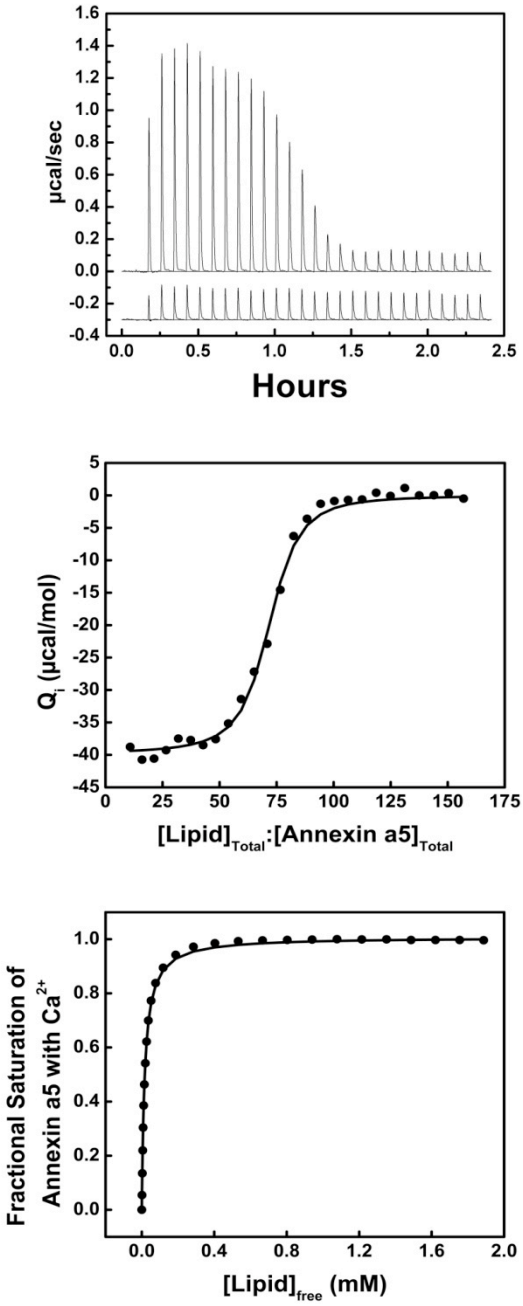

Figure 2.3: Results of the titration of 30 µM anx-a5 with lipid as LUVs made of a 60:40 mixture of POPC:POPS in the presence of 0.5 mM Ca^{2+} at 15°C. *Top:* Raw ITC data. *Middle:* Integrated heats of binding as a function of ligand to protein ratio. *Bottom:* Binding isotherm of fractional saturation as a function of free [Lipid].

Section 2.4: Discussion

A thermodynamic model seeks to capture the complexity of a binding process between anx-a5, membrane and Ca^{2+}. It reduces the dynamic conformational distribution of a protein to a distribution between two states, one in solution and one associated with the membrane. The protein does not exist in only two states; rather we assume that there are two primary distributions of similar energies. The differences in protein distributions correlate with a differentiation in Ca^{2+} affinities. This simplification allows the description of a binding process in terms of a minimal number of binding constants.

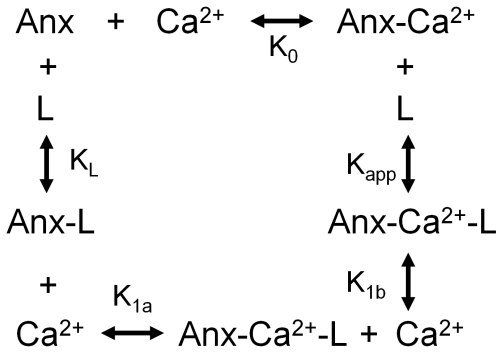

Figure 2.4: The thermodynamic cycle that describes the interactions between anx-a5 (Anx), Ca^{2+}, and lipid membranes (L).

The observed change in Ca^{2+} binding behavior upon addition of membrane suggests that the interactions between anx-a5 and both its ligands are linked through a thermodynamic cycle (Fig. 2.4). Thus, anx-a5's affinity for membrane in the presence of Ca^{2+} (K_{app}) can be described in terms of the different equilibrium constants describing Ca^{2+} binding (K_0, K_{1a}, and K_{1b}), the equilibrium constant describing lipid binding in the absence of Ca^{2+} (K_L), and free Ca^{2+} concentration as Eq. 2.3.

$$K_{app} = K_L * (1 + K_{1a}[Ca^{2+}])^2 (1 + K_{1b}[Ca^{2+}])^3 / (1 + K_0[Ca^{2+}])^5 \qquad (2.3)$$

Ca^{2+} binding affinity in the absence of membrane, K_0, is fairly similar to that of the three sites with low affinity, K_{1b}, in the presence of membrane. (In terms of free energy, this difference is negligible.) This allows the expression for K_{app} to be simplified to Eq. 2.4.

$$K_{app} = K_L * (1 + K_{1a}[Ca^{2+}])^2 / (1 + K_0[Ca^{2+}])^2 \quad (2.4)$$

Using this relationship, the affinity for anx-a5 to bind membrane in the absence of lipid was calculated to be $K_L = (3.6 \pm 0.8) \times 10^2\ M^{-1}$ ($K_{D,L} = 2.8 \pm 0.8$ mM).

Further information about Ca^{2+} free membrane binding by anx-a5 can be calculated using Hess's Law. Since the binding of both ligands are thermodynamically linked, the enthalpy required for anx-a5 to transition from the unbound state in solution to the fully saturated, Ca^{2+} and lipid bound state should be constant regardless of the path taken. This leads us to Eq. 2.5,

$$n_0 (\Delta H_0) + \Delta H_{app} = \Delta H_L + n_{1a} (\Delta H_{1a}) + n_{1b} (\Delta H_{1b}) \quad (2.5)$$

Where ΔH_L is the heat associated with binding lipid in the absence of Ca^{2+}. This is calculated to be -0.9 ± 0.2 kcal/mole, a value hardly detectable by ITC. In this way, the overall heat produced by three sides of the thermodynamic cycle suggest that the fourth is athermal, and in fact, membrane binding by anx-a5 in the absence of Ca^{2+} did not generate a measurable heat of interaction.

In order to adequately describe the data, the global fit to three sides of a thermodynamic cycle (Table 2.1) must result with an athermal fourth side of the cycle. In this way,

stringent discrimination of competing interaction models was possible. The proposed binding model was determined after systematically fitting the presented data sets with several binding models of increasing complexity (multiple sets independent sites, sequential binding sites, and various combinations of each, etc.). To reiterate, the three sides of the binding isotherm were fit by the same four binding constants (K_0, K_{1a}, K_{1b}, and K_L) to four sets of binding conditions (Ca^{2+} alone, Ca^{2+} in the presence of saturating membrane, membrane in the presence of saturating Ca^{2+}, and titrating membrane alone).

Table 2.1: Thermodynamic parameters describing anx-a5 binding interactions.

	Ca^{2+} Binding			Membrane Binding*
	Without Membrane	With Membrane, High Affinity	With Membrane, Low Affinity	With Saturating Ca^{2+} Present
n	5.0 ± 0.4	2.0 ± 0.1	3.0 ± 0.3	z = 69.7 ± 0.3
K (M^{-1})	3100 ± 300	100000 ± 10000	5600 ± 300	57000 ± 4000
K_D (μM)	330 ± 40	10 ± 2	180 ± 10	18 ± 1
ΔH (kcal/mol)	-2.4 ± 0.2	4.6 ± 0.2	-13.8 ± 1.4	-19.4 ± 0.1
$T\Delta S$ (kcal/mol)	2.2 ± 0.2	11.2 ± 0.3	-8.9 ± 1.4	-13.1 ± 0.1
ΔG (kcal/mol)	-4.6 ± 0.1	-6.6 ± 0.1	-4.9 ± 0.1	-6.2 ± 0.1

* The affinity for anx-a5 to bind membrane in the absence of lipid was calculated to be $K_L = (3.6 \pm 0.8) \times 10^2\ M^{-1}$ ($K_{D,L}$ = 2.8 ± 0.8 mM).

The presented model is a variation to a common theme in biological function [25-29]. This cooperative response is due to redistribution of the protein's conformational states, and for such a cooperative response, the basal state (ligand-free state of the protein) must predominate. Anx-a5 is in dynamic conformational equilibrium, and even in the absence of Ca^{2+}, some of the conformations are acquiescent to weakly associate with the membrane. Here we consider conformations in the allosteric transition sense, which need not be a

gross change in structure of the protein, rather, a subtle redistribution of conformers [8]. For anx-a5, whether in the solution state or in the membrane bound state, binding of Ca^{2+} is independent (the binding of one Ca^{2+} does not impact the binding of another Ca^{2+}). However, the conformers of the membrane associated anx-a5 have a greater affinity for Ca^{2+} than does the solution state conformers of the protein (see Fig. 2.5 for analogy to MWC model). Because the membrane bound state of the protein has a greater affinity for Ca^{2+} than solution state protein, upon introduction of Ca^{2+}, this state binds the cation with greater probability. This shifts the equilibrium, and more (Ca^{2+}-free) protein associates with the membrane. It is this membrane bound state of the protein that then binds more and more Ca^{2+}. If the protein was mostly or completely membrane bound, an independent (hyperbolic-shaped) Ca^{2+} binding response would result. However, if a relatively small population of the protein is membrane associated, in the absence of Ca^{2+}, a cooperative Ca^{2+} binding profile results. Upon a Ca^{2+} influx, the membrane-associated population of protein binds Ca^{2+}, and is therefore depleted, with a greater probability than the solution state. The membrane-associated (and Ca^{2+}-free) state is then becomes repopulated by a shift in equilibrium, giving the appearance of a plateau in Ca^{2+} binding (due to the shifting and replenishing). The more abrupt rise in fractional saturation of Ca^{2+} sites is due to the higher affinity of the membrane-associated state (compared to solution state affinity). This results in the characteristic sigmoidal binding profile of a cooperative binding response. The protein will transition from an unbound to bound state over a smaller concentration range of Ca^{2+} than in an independent Ca^{2+} site binding scenario. Thus, if a protein with multiple binding sites has one affinity for a ligand when membrane bound and another affinity when in the solution (aqueous) state, this protein will exhibit cooperative binding. This is only true if the membrane bound state of the protein is populated to a relatively low extent in the absence of the ligand. This suggests that in order to achieve switch-like binding of a ligand

at the membrane, weak membrane association in the absence of that ligand is one means to attain this response.

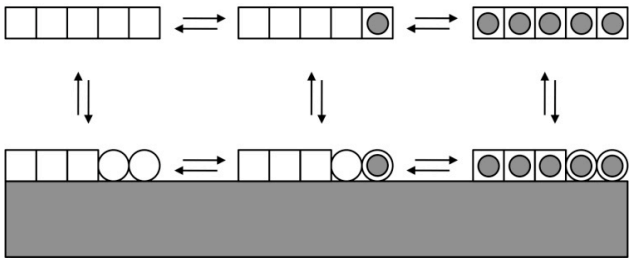

Figure 2.5: Schematic extension of the MWC model of binding. Five Ca^{2+} ions are bound by anx-a5 where the MWC states, Tensed (T) and Relaxed (R), are replaced by solution and membrane-bound states. In the absence of membrane, all five sites are exothermic with low affinity (represented as squares). In the presence of membrane, the five Ca^{2+} binding sites differentiate into two classes – three low affinity exothermic sites and two high affinity endothermic sites (represented as circles). As in the classic MWC model, in each state, solution or membrane-bound, binding of ligand is independent between the sets of sites.

Using the heat of binding, cooperative ligation of Ca^{2+} by anx-a5 was found to depend on the association of the protein with the membrane (see Fig. 2.1 and 2.2, bottom panels). To illustrate this interdependence, the fraction of each state of the protein (free, bound to Ca^{2+} in solution, bound to Ca^{2+} and membrane, or bound only to membrane) as predicted by the experimentally determined association constants was plotted as a function of total Ca^{2+} concentration. By varying the total membrane concentration in these predictions, increasing Ca^{2+} was shown to redistribute the protein between either being in solution or being associated with the membrane to varying degrees (Fig. 2.6). If this initial membrane association in the absence of Ca^{2+} was too weak, such as when the theoretical membrane concentration is low (0.2 mM total lipid, as in Fig. 2.6, top panel), the protein remains predominantly in the solution state that is Ca^{2+} bound, even at high concentrations of Ca^{2+}. If the theoretical lipid concentration is high (20 mM total lipid, as in Fig. 2.6, middle panel),

the protein is bound predominantly to both Ca^{2+} and the membrane. The binding of Ca^{2+} in either case is not cooperative.

However, the total membrane concentration at which our experimental results (presented in Fig. 2.1, 2.2, and 2.3) were obtained resides between these scenarios (2 mM total lipid, as in Fig. 2.6, bottom panel). This creates an exquisitely sensitive response, as evidenced by the redistribution of the protein over a very small concentration range of Ca^{2+} from being only Ca^{2+} bound in solution to the Ca^{2+} and membrane bound state (see Fig. 2.2, bottom panel for membrane and Ca^{2+} bound state). Note that the fraction of protein associated with the membrane in the absence of Ca^{2+} is not very significant (approximately 20%, see Fig. 2.6, bottom panel, dashed line y-intercept), yet the switching between being bound to Ca^{2+} alone or to both membrane and Ca^{2+} is strongly modulated by this membrane, (yet calcium-ion free) association. We suggest that this switching is physiologically relevant, as it provides a sensitive means of communicating binding information.

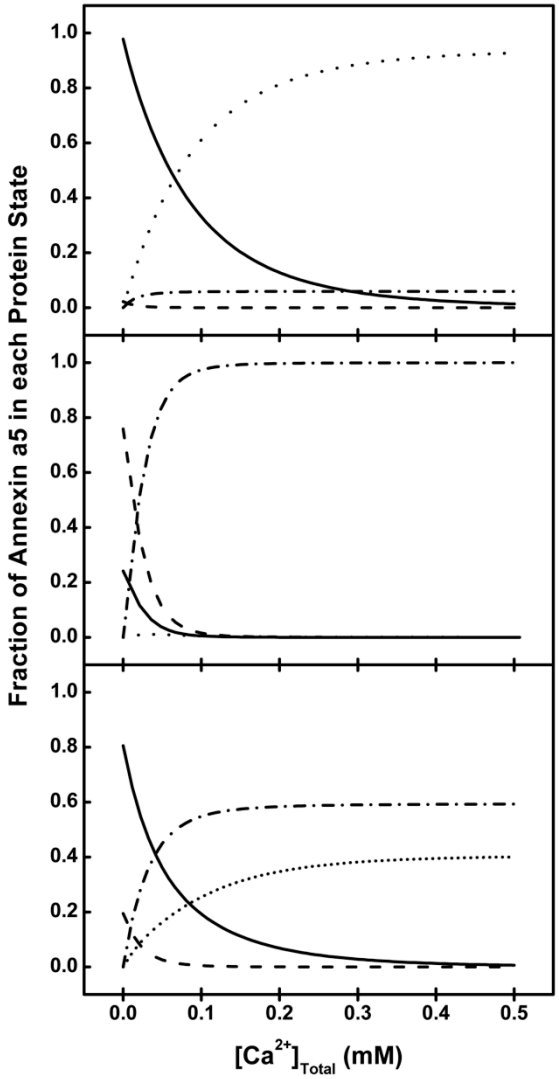

Figure 2.6: Distribution of all possible states of anx-a5 as a function of increasing concentrations of Ca^{2+}. *Solid Line:* Ligand free protein, *Dotted Line:* Ca^{2+}-bound protein, *Dashed Line:* Lipid-bound protein, *Dot-Dash Line:* Ca^{2+} & Lipid-bound protein. Distributions were calculated using the binding constants in Table 2.1 for 24 μM anx-a5 assuming a decreased total lipid concentration of 0.2 mM (Top), an increased total lipid concentration of 20 mM (Middle), or the experimental conditions of 2 mM total lipid (Bottom). Lipids were LUVs composed of a 60:40 ratio of POPC:POPS.

To further illustrate the sensitivity, and how weak membrane association conveys cooperativity, the binding isotherms of Fig. 2.1 and 2.2 (bottom panels) are overlapped (Fig. 2.7). The impact of membrane association becomes apparent as more of anx-a5 is saturated with Ca^{2+} at a given calcium concentration when membrane associated compared to the solution state. The Ca^{2+} saturation exhibits the classic plateau and rise of a cooperative binding process where over a small Ca^{2+} concentration range of 100 μM, the fraction saturation of the protein changes from only 20% to 40% bound when in the presence of membrane. This is very similar to our previous finding with anx-a5 utilizing the Ca^{2+} mimic, Tb^{3+} [8]. The primary difference between this work and the previous work is a stronger protein-cation affinity (K_0), the affinities for cation are differentiated from K_1 to K_{1a} and K_{1b}, and in the use of a protein-lipid ratio of only 20 lipids/protein. The first difference may be due to the greater charge density of terbium ion compared to Ca^{2+}, which is the result of having similar ionic radius but different charges. The second difference is discernable via the differences in sign of heats of interaction upon Ca^{2+} ligation revealed by ITC. The third is an underestimation of the protein to lipid ratio, leading to an overestimation of the K_L as there will be a greater concentration of free lipid per bound protein.

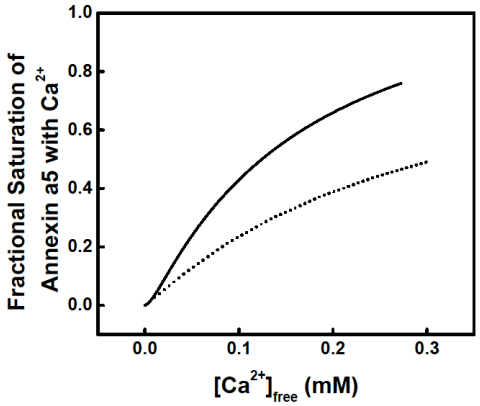

Figure 2.7: Overlay of the binding isotherms for Ca^{2+} for anx-a5 in both the solution state (dotted line) and membrane bound (solid line) states.

This provides a conceptual basis as to why weak membrane association is the basis of a cooperative response [9, 30-34]. It is only within the context of a thermodynamic cycle that such a result has meaning, that the insignificance of this interaction is significant. To respond with maximal sensitivity, biological systems must teeter at the precipice so that very little change in local concentration of ligand, here Ca^{2+}, is necessary to enact dramatic change in the population of the bound state of the protein, a mark of responsiveness of the system. We suggest that the membrane creates such a cusp and that the dynamic state of the membrane by virtue of the malleable nature of lipid-lipid interactions [3, 35] exists to position membrane associated proteins to react.

CHAPTER 3: LIGAND INDUCED CONFORMATIONAL REDISTRIBUTION IN SYNAPTOTAGMIN I C2A

Section 3.1: Introduction

The nervous system serves as a network for communication, sending instructions to every part of the body. Often, these signals must travel from one nerve cell to another by crossing the gap between them, the synaptic cleft. Communication across this gap is achieved via the release of neurotransmitter molecules from the pre-synaptic neuron, which reach receptors on the post-synaptic neuron by diffusion. The evoked release of these signaling molecules is achieved through regulated exocytosis in the pre-synaptic neuron that is triggered by an influx of Ca^{2+} [36-37]. Despite the fact that the role of this Ca^{2+} influx is well understood, controversy still exists in defining a detailed mechanism by which this signal is transduced into synchronous release of neurotransmitter molecules by regulated exocytosis.

Several proteins are known to participate in neuronal regulated exocytosis, perhaps most notably the soluble N-ethylmaleimide sensitive factor attachment protein receptor complex (or SNARE complex) made of synaptobrevin, syntaxin, and SNAP-25. One other class of proteins, the synaptotagmins, is also a key participant in both neurotransmitter release and the associated controversy. In particular, one member of the synaptotagmin family, Synaptotagmin I (Syt I), has been shown to serve as the primary Ca^{2+}-sensor for regulated exocytosis in neurons [36-37]. Structurally, Syt I is made of two C2 domains, dubbed C2A and C2B, that are tethered to the membrane by a transmembrane helix. These domains are able to bind two ligands, Ca^{2+} and acidic phospholipids (such as phosphatidylserine) [11]. Of the two domains, the C2A domain

has specifically been shown to exhibit high sensitivity to changes in Ca^{2+} concentration. This domain has three Ca^{2+} binding sites clustered together on the lipid-facing tip of the domain. In the absence of lipid, the third site has millimolar affinity for Ca^{2+}; in the presence of lipid, however, this site's ability to bind Ca^{2+} is dramatically increased [7, 38]. As the calcium sensor in regulated exocytosis, this sensitivity is fundamentally necessary for function, as the ability to quickly respond to the Ca^{2+} signal could literally mean the difference between life and death.

Syt I has been intensely studied, yet mystery still remains over the exact details of the mechanism by which the Ca^{2+} signal is transduced into an exocytosis event. In order for this protein to be responsive to changes in the concentrations of Ca^{2+}, some sort of change in response to binding is necessary. However, no large-scale structural changes are observed upon introduction of ligand in previous NMR studies [39]. Recently, iterative targeted mutations meant to restore specific residues in a chimeric Syt I-Syt VII hybrid were unable to rescue Syt I function *in vivo*. These results suggested that even subtle sequence and structural differences between synaptotagmin mutants could be responsible for the observed functional variation [40]. Bulk vesicle fusion assays have shown an increase in SNARE-driven vesicle fusion upon addition of Syt I and Ca^{2+}, but the timescales (minutes to hours) of these fusion experiments were still much slower than physiological timescales (2ms) [41]. Furthermore, single vesicle docking and fusion assays revealed several heterogeneous pathways for both vesicular docking and fusion; however, the molecular basis and physiological significance of this functional diversity remains unresolved [42].

The myriad observations suggest the following hypothesis; Syt I must exist in different forms to function – at the very least, there must exist an "on" state and an "off" state (one that is able to initiate assembly of the SNARE complex to promote vesicle docking and fusion, and one that cannot) – and that it must be able to quickly transition between these forms in response to changes in Ca^{2+} concentration. This diverse range of states could be described as an overall distribution of conformers, and within this overall distribution there would exist subsets of states that would be binding-competent for the ligands: Ca^{2+}, phospholipids, or both. There would also exist a subpopulation of states that would be physiologically active (that is, capable of initiating synchronous neurotransmitter release).

When determining the extent to which the protein actually samples each of these possible conformers, we must consider the overall energetics of the system. Under a given set of conditions, the protein will redistribute how it populates each of its possible states until it minimizes the overall free energy of the system. Thus, by determining the energetics associated with the C2A domain in the absence and presence of its ligands, we are able to gain insight into how the distribution of conformers responds to changes in cellular conditions. Specifically in the case of Syt I C2A, this conformational redistribution must be exquisitely sensitive to small changes in Ca^{2+} concentrations, as well as easily reversible. (Note that the ability to "turn off" neurotransmitter release is equally as important.) This level of responsiveness suggests that the interactions involved must be weak.

According to this model, if strong, rigid interactions were to maintain a protein's structure, it would not be as sensitive to small changes in ligand concentration. If

instead, the protein's structural interactions were weak, the protein would exhibit greater sensitivity to changes in its environment [43-44]. This model for the mechanism of sensitivity is particularly insightful when applied in the context of the previously mentioned Syt I studies because it is capable of unifying these otherwise unexplainable observations. In all cases, minute differences between the various samples under study were found to have relatively impactful consequences.

Using differential scanning calorimetry (DSC) and fluorescence lifetime spectroscopy (FLT) to monitor the denaturation, the magnitudes of the interactions stabilizing the C2A domain of Syt I in the presence and absence of saturating concentrations of its ligands were ascertained. Our data is consistent with the concept that a responsive system, such as the C2A domain, is held together by overall weak interactions. This provides a molecular basis for transmuting the Ca^{2+}-influx into the physiological response of evoked release of neurotransmitters through regulated exocytosis.

Section 3.2: Materials and Methods

Subsection 3.2.1: Materials

Both 1-palmitoyl-2-oleoyl-sn-glycero-3-phosphocholine (POPC or 16:0,18:1PC) and 1-palmitoyl-2-oleoyl-sn-glycero-3-phospho-L-serine (POPS or 16:0,18:1PS) were obtained from Avanti Polar Lipids, Inc. (Birmingham, AL). Potassium chloride (KCl) was Puriss-grade and 3-(N-morpholino)propanesulfonic acid (MOPS) was Biochemika grade from Fluka Chemical Corp. All buffers used were decalcified using Chelex-100 ion-exchange resin (Bio-Rad Labs).

Subsection 3.2.2: Purification of Human Syt I C2A

Human Syt I C2A was purified as a glutathione S-transferase (GST) fusion protein using affinity chromatography, followed by removal of the GST domain. The KG-C2A [140-265] plasmid was transformed into BL21-DE3 competent *Escherichia coli* cells and the DNA was sequenced (Northwoods DNA, Inc., Bemidji, MN). 5.0 ml starter cultures in LB Broth (overnight growth at 37°C) were used to inoculate 1 L LB Broth cultures. These 1 L cultures were incubated at 37°C in the presence of 100 µg/ml ampicillin until an optical density of 0.8-1.4 was reached (~5 hr). After induction with 1.0 mM isopropyl-β-D-thiogalactopyranoside, the cultures were incubated at 37°C for an additional 5 hr. The cells were harvested by centrifugation. 20 g of the cell pellet was lysed by sonication in 20 mM MOPS, 100 mM KCl, pH 7.5 using Complete EDTA-free protease inhibitor tablets (Roche). Following lysis, cellular debris was pelleted by centrifugation (30 min at 16,000 rpm). The supernatant was treated with benzonuclease (10 units/ml in the presence of 5.0 mM magnesium chloride) for at least 8 hr. Host DNA was separated by centrifugation (45 min at 20,000 rpm) followed by sterile filtering with a 0.4 µm filter. The C2A-GST fusion protein was allowed to bind 50.0 ml of equilibrated GST-affinity resin for 2 hr at

4°C. Elution of nonspecific host proteins was achieved using 500 ml of lysis buffer. (Complete elution was confirmed by monitoring the A280 via Nanodrop (Thermo Scientific).) The media was re-suspended using 30 ml of 6.0 µg/ml thrombin solution (in lysis buffer) and allowed to rock at room temperature for 6 hr. After cleavage of the GST domain, free C2A and thrombin were eluted from the column with lysis buffer. (Again, complete elution was confirmed by monitoring the A280.) The protein solution was rocked overnight in the presence of 2 µl/ml p-aminobenzamidine-agarose media (Sigma) to remove thrombin; the media was then separated from the protein solution by centrifugation (15 min at 3000 rpm) and sterile filtering with a 0.4 µm filter. The resulting protein solution was repassed over a clean GST-resin column as needed to ensure separation of any contaminating GST. Recombinant C2A was dialyzed in the presence of Chelex-100 resin to remove any contaminating Ca^{2+} by batch method and concentrated to ~50 µM using concentrator units (Amicon) with a 10 kDa cutoff. Final purity was determined to be >95% by SDS-PAGE densitometry. Final concentrations were determined using a Nanodrop with an A280 extinction coefficient of 12090 $cm^{-1}M^{-1}$.

Subsection 3.2.3: Preparation of Lipid Vesicles

Vesicles were prepared via extrusion as described in Subsection 2.2.3 in this thesis.

Subsection 3.2.4: Differential Scanning Calorimetry (DSC)

DSC experiments were performed on a NanoDSC (TA Instruments, New Castle, DE) using protein concentrations of approximately 0.2 mg/ml and a scan rate of 1°C/min. These scans were conducted in 20 mM MOPS, 100 mM KCl, pH 7.5 which was chelexed to remove any trace Ca^{2+}. Those scans performed in the absence of Ca^{2+} contained 500 µM EGTA to further ensure Ca^{2+}-free conditions. Runs in the presence of

Ca^{2+} used concentrations such that the protein's Ca^{2+}-binding sites were 95% saturated (calculated using binding constants determined for terbium ion as in Kertz et al. [7]. Runs in the presence of lipid membranes were designed to contain an excess of negatively charged phospholipids. The phospholipids were prepared as LUVs composed of a 60:40 mixture of 16:0,18:1PC and 16:0,18:1PS. 60%-90% reversibility was found by repeating the scan. (Displaying reversibility was important, as it allowed the data to be analyzed using reversible thermodynamics.)

Subsection 3.2.5: Fluorescence Lifetime Spectroscopy (FLT)

FLT experiments were performed on a Lifetime Spectrometer (Fluorescence Innovations, Inc., Bozeman, MT) using protein concentrations of 0.03 mg/ml. These scans were conducted in chelexed 20 mM MOPS, 100 mM KCl, pH 7.5. The intrinsic fluorescence lifetime of the C2A's endogenous tryptophan was monitored as a function of increasing temperature in 2°C increments. The spectrometer is specifically tuned to excite at 295 nm (the excitation maxima of a tryptophan residue), allowing for uniquely sensitive detection of changes in the fluorescence lifetime signal. An emission spectrum was collected from 310 nm to 360 nm, and data collected at 340 nm was used in the analysis. This wavelength had the strongest contribution from tryptophan with little contribution from water fluorescence. Changes in the fluorescence lifetime emission at other wavelengths were separately analyzed to confirm the data collected at 340 nm was representative of the signal change associated with the unfolding transition. The collected wavelengths were then replotted to recapitulate the steady state fluorescence emission spectrum, further confirming the veracity of the approach. When applicable, a background of 500 μM EGTA was used to ensure Ca^{2+}-free conditions. In runs containing Ca^{2+}, concentrations corresponded to 95% saturation [7]. Runs in the

presence of lipid membranes were designed to contain an excess of negatively charged phospholipids. The phospholipids were prepared as LUVs composed of a 60:40 mixture of 16:0,18:1PC and 16:0,18:1PS. Reversibility was shown by comparing the fluorescence lifetime intensity after cooling the sample to the initial temperature of the scan (80%-90% for lipid-free conditions, 60%-70% when lipid is present).

Section 3.3: Results

Protein unfolding, in some cases, can be simplified to a two-state transition between native (N) and denatured (D) protein macromolecules with no unfolding intermediates. In such a model, a mass balance equation describing the total concentration of protein macromolecules ($[P_T]$) could be expressed as Eq. 3.1.

$$[P_T] = [N] + [D] \tag{3.1}$$

The unfolding transition can be described by an equilibrium constant $K = [D]/[N]$. Furthermore, expressions for the fraction of protein in each state (native or denatured) in terms of this equilibrium constant can be derived as shown in Eq. 3.2 (native fraction) and Eq. 3.3 (denatured fraction).

$$f_N = [N]/[P_T] = 1/(1 + K) \tag{3.2}$$

$$f_D = [D]/[P_T] = K/(1 + K) \tag{3.3}$$

Where f_N and f_D represent the fractions of native and denatured protein, respectively. Describing these fractions in terms of the equilibrium constant (K) is of particular use because it can be further related to Gibbs free energy (ΔG), which can be thought of as the capacity to do chemical work. This is achieved via the Eq. 3.4, where R represents the ideal gas constant and T represents temperature in Kelvin.

$$\Delta G = -RT\ln K \tag{3.4}$$

The Gibbs free energy associated with a system under a given set of conditions can further be dissected into enthalpic (ΔH) and entropic (ΔS) contributions as Eq. 3.5.

$$\Delta G(T) = \Delta H(T) - T\Delta S(T) \quad (3.5)$$

Where $\Delta H(T)$ and $\Delta S(T)$ are the temperature dependent functions of the enthalpy and entropy, respectively, describing the unfolding transition. At the midpoint of this transition, the point where [N] = [D], this expression for $\Delta G(T)$ simplifies to zero. The temperature where this occurs (referred to hereafter as T_m) is a useful reference temperature, from which extrapolation of the thermodynamic parameters to more physiologically relevant temperatures is possible. This extrapolation is achieved by describing $\Delta H(T)$ and $\Delta S(T)$ in terms of the reference state thermodynamics as Eq. 3.6 and Eq. 3.7, respectively.

$$\Delta H(T) = \Delta H_{Tm} + \Delta C_p\,(T - T_m) \quad (3.6)$$

$$\Delta S(T) = \Delta H_{Tm}/T_m + \Delta C_p(\ln(T/T_m)) \quad (3.7)$$

Where ΔH_{Tm} represents the enthalpy associated with the transition and ΔC_p represents the change in heat capacity between the native and denatured states of the protein (assumed in this analysis to be temperature independent). Thus, the Gibbs free energy associated with the denaturation process at any temperature can be calculated in terms of three parameters (ΔH_{Tm}, T_m, and ΔC_p) as Eq. 3.7.

$$\Delta G(T) = \Delta H_{Tm}\,(1 - T/T_m) + \Delta C_p\,(T - T_m - T\ln(T/T_m)) \quad (3.8)$$

In the DSC experiments (Fig. 3.1, Panels A-D), the heat capacity of a protein sample is measured against a reference solution containing no protein. As the temperature increases, the protein's higher order structure absorbs heat, causing it to denature. The excess heat necessary to drive the protein through the phase transition of unfolding is measured by the calorimeter as a differential heat capacity as a function of temperature ($C_p(T)$). After correcting for the pre-transitional baseline, this differential measurement can be described for a two-state transition in terms of the enthalpy associated with the transition ($\Delta H(T)$) and the fraction of the protein that has gone through the transition (f_D) as Eq. 3.9.

$$C_p(T) = \mathrm{d}/\mathrm{d}T\,(\Delta H(T)\, f_D) \qquad (3.9)$$

Note that both $\Delta H(T)$ and f_D can, with simple substitutions, be expressed in terms of the reference state thermodynamic parameters, ΔH_{Tm}, T_m, and ΔC_p.

In the FLT experiments (Fig. 3.1, Panels E-H), the fluorescence lifetime emission of Syt I C2A's endogenous tryptophan was measured. Tryptophan's fluorescence lifetime is highly sensitive to its local chemical environment. As the protein transitions from the native to denatured state, the local environment surrounding the tryptophan changes. This causes a corresponding change in the fluorescence lifetime signal associated with the native state (S_N) and denatured state (S_D). Thus, the area of the fluorescence lifetime decay peak was monitored as a function of temperature, as the integral of the FLT curve is the intensity. The observed composite signal, $S(T)$, representing the transition between two states as a function of temperature was related to an equilibrium constant by Eq. 3.10.

$$S(T) = S_D + (S_N - S_D)/(1 + K) \quad (3.10)$$

Where signal associated with the native and denatured states were assumed to be linear and thus described as $S_N = m_N\ T + b_N$ and $S_D = m_D\ T + b_D$ [45]. Note that $S(T)$ is described in terms of the equilibrium constant K. As with the DSC, this data can therefore, with simple substitutions, be expressed in terms of the reference state thermodynamic parameters, ΔH_{Tm}, T_m, and ΔC_p.

Since both experimental techniques monitored the same transition, DSC and FLT data were fit simultaneously by non-linear least squares regression analysis using ΔH_{Tm}, T_m, and ΔC_p as global fitting parameters [46]. Four replicates of each technique (for a total N = 8) were used for each ligand condition (ligand-free, in the presence of saturating Ca^{2+}, in the presence of excess phospholipid, and in the presence of both Ca^{2+} and phospholipid). Error associated with the regression was determined using an approach by De Levie [47].

Table 3.1: Thermodynamic Parameters Describing Syt I C2A Denaturation

	ΔH (kcal/mole)	ΔS (kcal/moleK)	ΔC_p (kcal/moleK)	T_m (°C)	$\Delta G_{37°C}$ (kcal/mole)
Ligand-Free	58.7±0.3	0.18±0.01	1.9±0.1	56.0±0.1	2.32±0.05
Ca^{2+}	77.4±0.6	0.23±0.01	1.9±0.1	67.6±0.1	4.23±0.05
Phospholipid	61.3±1.1	0.19±0.02	1.9±0.1	55.5±0.2	2.44±0.05
Ca^{2+} & Phospholipid	72.4±0.9	0.21±0.01	1.9±0.1	75.6±0.3	3.73±0.05

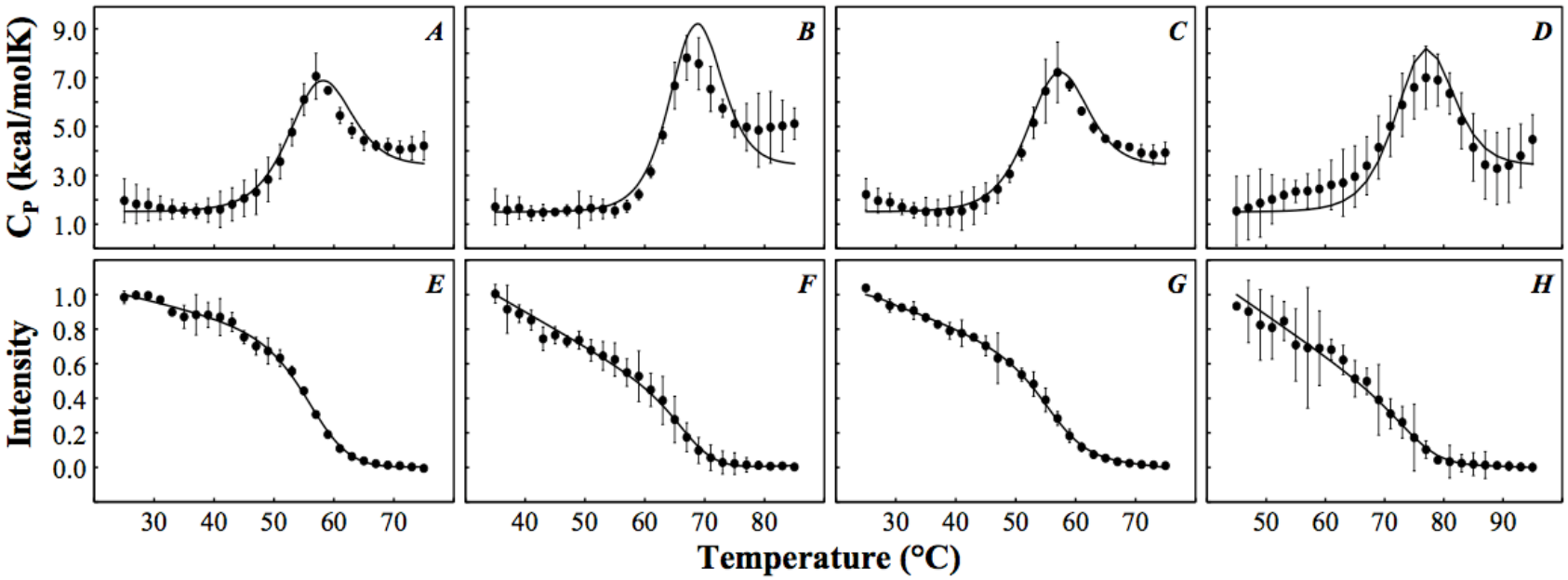

Figure 3.1: Denaturation of Syt I C2A. The data points represent the average of four trials (error bars show 95% confidence intervals based on four replicate experiments). The fit lines represent the results of a global fit of DSC and FLT experiments using the same set of parameters (Table 3.1). DSC experiments were run with 13 μM Syt I C2A in the presence of 500 μM EGTA (*Panel A*), 800 μM Ca^{2+} (representing 95% saturation) (*Panel B*), 870 μM total phospholipid (LUVs of 60:40 POPC:POPS) and 500 μM EGTA (*Panel C*), and 800 μM Ca^{2+} (representing 95% saturation) and 870 μM total phospholipid (LUVs of 60:40 POPC:POPS) (*Panel D*). FLT experiments were run with 0.75 μM Syt I C2A in the presence of 500 μM EGTA (*Panel E*), 770 μM Ca^{2+} (representing 95% saturation) (*Panel F*), 50 μM total phospholipid (LUVs of 60:40 POPC:POPS) and 500 μM EGTA (*Panel G*), and 770 μM Ca^{2+} (representing 95% saturation) and 50 μM total phospholipid (LUVs of 60:40 POPC:POPS) (*Panel H*).

Of the three global parameters, it was observed that ΔC_p was the most loosely constrained by the fit. This was likely due to the high level of variation in the DSC baseline associated with denatured protein, especially in the presence of Ca^{2+}. (Also, this parameter did not have a significant impact on the overall shape of the calculated FLT fit line. Therefore, the FLT datasets provided little or no additional constraint on the parameter.) Fortunately, in the absence of all ligands, the fitted ΔC_p value was in good agreement with a theoretical value [48]. Thus, to constrain the fits in the presence of ligand, the ΔC_p was assumed to be constant across all ligand conditions. The resulting global parameters, as well as the Gibbs free energy of stability extrapolated to physiological temperature ($\Delta G_{37°C}$) are shown in Table 3.1.

Section 3.4: Discussion

Overall, the Gibbs free energy associated with the denaturation of Syt I C2A was found to be quite low in both the presence and absence of all ligands when compared to proteins of similar size [49]. This result is consistent with the hypothesis that, as a means to be responsive, the C2A domain must be stabilized by weak interactions. In the absence of ligand, such a system could breathe and flex through a wide range of conformers, and the extent to which the protein sampled each possible conformer would be determined by its associated free energy. Within this distribution of conformers, a subset of them would be binding-competent for a ligand. Upon introduction of this ligand, the free energy associated with these conformers would decrease such that any binding-competent conformations would be stabilized. This would cause an overall redistribution in the statistical likelihood of existing in *all* of the possible protein conformations, not just those that are binding-competent. This redistribution is made easier by the overall weak energetics and allows for communication between both the conformational and binding equilibria.

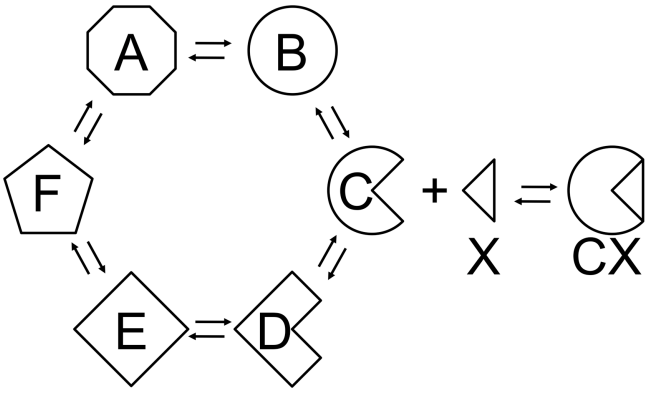

Figure 3.2: Linked conformational and binding equilibria: a schematic of a simplified version of this general model. A-F represents different conformers; X represents ligand.

Thought of another way, you can imagine a protein that exists as a distribution of six different conformations (A-F), each with its own associated free energy. These six conformers would be in dynamic equilibrium with one another. Also, imagine that of the six, only conformer C is binding competent for ligand X. (Such a system is diagrammed in Fig. 3.2.) By introducing ligand X, the binding equilibrium will shift, driven by Le Chatelier's Principle, such that more of the CX complex will be formed. A side effect of this shifting is a depletion of the free C conformation that is not bound to X. Thus, the conformational equilibria between states A-F will shift to compensate, and the ligand-free form of the C conformer will be repopulated. Thus, the statistical likelihoods of existing in all of the states, not just those able to bind ligand X, are impacted by introduction of ligand X. Furthermore, as the protein approaches saturation with ligand X, the equilibrium is shifted such that the protein essentially exists only as conformer C, the state that is binding competent. In this way, introduction of ligand can select for and stabilize a subset of the overall distribution of conformer states.

We suggest that it is this linkage between ligand binding and conformational redistribution that is the key to the C2A domain of Syt I's functionality. We propose a model where the C2A domain samples a wide distribution of conformations, and only a subset of these conformers could have important physiological ramifications, such as to initiate vesicle docking and fusion through SNARE complex assembly. In the absence of Ca^{2+}, the probability of existing in these active states is low, but not zero. Thus, these conformations would be populated to some degree with little to no Ca^{2+} present, but only to an extent that is below the physiological threshold required to trigger an evoked response. Furthermore, in order for the other proteins involved in the fusion machinery to be responsive to minute changes in Syt I, they too are likely to be dominated by weak

interactions. Thus, the SNARE complex could exist as a distribution of states, sampling a fusion-competent state with nonzero probability in the absence of Ca^{2+} stimulation. This provides a molecular mechanism for the random, spontaneous release of neurotransmitter observed in the absence of an action potential in neurons.

Upon introduction of Ca^{2+}, the likelihood of existing in a given state would shift such that binding-competent conformers are stabilized. However, if we assume that within the Ca^{2+} binding-competent subset there is an increased likelihood of the protein being physiologically active, then the overall conformational redistribution driven by Ca^{2+}-influx would also increase the probability of existing in the active state. If this redistribution readily occurs in response to small changes in Ca^{2+} concentrations, then the resultant increase in conformers able to trigger SNARE-driven fusion would be sufficient to cause synchronous neurotransmitter release. This conformer redistribution, therefore, must be highly responsive, a property made possible by the overall weak energetics associated with transitioning from one conformer to another. This allows small perturbations in intracellular Ca^{2+} concentrations to have a much more dramatic effect on the distribution of states.

This hypersensitivity to intracellular conditions not only reveals the thermodynamic underpinnings of Syt I C2A's function, but it also helps to rectify some of the aforementioned unexplainable observations of the field. Introduction of any sort of mutation into wild type Syt I would result in redefining the overall set of possible interactions, thus redefining the distribution of states; this would dramatically alter the energetics of the system and, by extension, the ability of Syt I to function. This is further supported by every point mutation in Syt I being constitutively lethal to the embryo,

implying that *all* residues are important to function. Also, a system controlled by an ensemble of weak interactions would be expected to be more sensitive to any intrasample heterogeneity in single vesicle docking experiments. In bulk *in vitro* vesicle docking assays where one or more of the important factors for regulated exocytosis are missing, fusion-competent conformers may be incompletely stabilized. Thus, while fusion would still be possible, the kinetics would be expected to be much slower. In this way, these seemingly unexplainable and unrelated phenomena can be unified using the same predictive model.

We observe the expected stabilization in Gibbs free energy at physiological temperature upon introduction of Ca^{2+} in Syt I C2A that is predicted by this model. In the presence of phospholipid membranes, however, the change in stabilization is hardly detectable. This result could be attributed to the differences between the two ligands: Ca^{2+} binding would require specific interactions with the coordination sphere of the cation. Conversely, membrane binding is much less specific; the lipids within a membrane are constantly redistributing to minimize their own free energy. Thus, as no membrane surface would be alike, a protein must retain some flexibility (and therefore, a low overall free energy) to interact with such a dynamic surface. In the ternary complex (C2A bound to Ca^{2+} and membrane), we again observe a stabilization of a subset of the overall distribution, though not as pronounced as in solution alone.

A limitation of this work is the use of the two-state assumption to fit such a conformationally diverse system. While seemingly counterintuitive, this approximation is valid for Syt I C2A if we define these two states (native and denatured protein) not as singular conformations, but rather as distributions of conformers with similar energetics.

In this way, we are able to describe the data while circumventing the mathematical complications associated with more complex models. Furthermore, to justify this simplification, it is common practice to compare the fitted enthalpy value (ΔH_{Tm}) with the V'ant Hoff enthalpy (ΔH_{VH}) found by integrating the DSC data as a function of temperature. For ligand-free conditions and both conditions with lipid present, these values are within statistical agreement of one another. In the presence of only saturating Ca^{2+} (in the absence of membrane), these two enthalpy values are statistically different, but this is more likely a result of either the variation within the post-transition baseline in the DSC data or the observed irreversibility associated with these conditions. Thus, we propose that this model is more than sufficient for describing the system.

We hypothesized that in order to serve as the calcium sensor for regulated exocytosis, Ca^{2+} binding must trigger the assembly of the components conducive to fusion. One mechanism to achieve this ability would be for a protein to have a low free energy of stability. We propose that C2A of Syt I is able to act as the Ca^{2+} sensor for regulated exocytosis via a ligand-induced energetic redistribution of conformers made possible by overall weak energetics. This mechanism provides the thermodynamic basis for stabilizing a subset of states from its overall conformational distribution. Furthermore, we suggest that this stabilization leads to increased population of those conformers that are able to promote fusion by assembling the factors necessary to initiate evoked release of neurotransmitters through SNARE-driven fusion.

REFERENCES:

1. Berg, J.M., J.L. Tymoczko, and L. Stryer, *Biochemistry*. 6th ed. 2007, New York: W.H. Freeman. 1 v. (various pagings).
2. Singer, S.J. and G.L. Nicolson, *The fluid mosaic model of the structure of cell membranes.* Science, 1972. **175**(23): p. 720-31.
3. Almeida, P.F., A. Pokorny, and A. Hinderliter, *Thermodynamics of membrane domains.* Biochim Biophys Acta, 2005. **1720**(1-2): p. 1-13.
4. Jacobson, K. and C. Dietrich, *Looking at lipid rafts?* Trends Cell Biol, 1999. **9**(3): p. 87-91.
5. Hinderliter, A., et al., *Domain formation in a fluid mixed lipid bilayer modulated through binding of the C2 protein motif.* Biochemistry, 2001. **40**(13): p. 4181-91.
6. Vats, K., et al., *Peripheral protein organization and its influence on lipid diffusion in biomimetic membranes.* ACS Chem Biol, 2010. **5**(4): p. 393-403.
7. Kertz, J.A., et al., *The cooperative response of synaptotagmin 1 C2A. A hypothesis for a Ca2+-driven molecular hammer.* Biophys J, 2007. **92**: p. 1409-1418.
8. Almeida, P.F., et al., *Allosterism in membrane binding: a common motif of the annexins?* Biochemistry, 2005. **44**(32): p. 10905-13.
9. Torrecillas, A., et al., *Calorimetric study of the interaction of the C2 domains of classical protein kinase C isoenzymes with Ca2+ and phospholipids.* Biochemistry, 2004. **43**(37): p. 11727-39.
10. Davis, D.B., et al., *Calcium-sensitive phospholipid binding properties of normal and mutant ferlin C2 domains.* J Biol Chem, 2002. **277**(25): p. 22883-8.
11. Sutton, R.B., et al., *Structure of the first C2 domain of synaptotagmin I: a novel Ca2+/phospholipid-binding fold.* Cell, 1995. **80**: p. 929-938.
12. Raynal, P. and H.B. Pollard, *Annexins: the problem of assessing the biological role for a gene family of multifunctional calcium- and phospholipid-binding proteins.* Biochim Biophys Acta, 1994. **1197**(1): p. 63-93.
13. Concha, N.O., et al., *Rat annexin V crystal structure: Ca(2+)-induced conformational changes.* Science, 1993. **261**(5126): p. 1321-4.
14. Murphy, J., K. Knutson, and A. Hinderliter, *Protein-lipid interactions role of membrane plasticity and lipid specificity on peripheral protein interactions.* Methods Enzymol, 2009. **466**: p. 431-53.
15. Hinderliter, A., R.L. Biltonen, and P.F. Almeida, *Lipid modulation of protein-induced membrane domains as a mechanism for controlling signal transduction.* Biochemistry, 2004. **43**(22): p. 7102-10.
16. Moss, S.E. and R.O. Morgan, *The annexins.* Genome Biol, 2004. **5**(4): p. 219.
17. Babiychuk, E.B. and A. Draeger, *Annexins in cell membrane dynamics. Ca(2+)-regulated association of lipid microdomains.* J Cell Biol, 2000. **150**(5): p. 1113-24.
18. Lemmon, M.A., *Membrane recognition by phospholipid-binding domains.* Nat Rev Mol Cell Biol, 2008. **9**(2): p. 99-111.
19. Morgan, R.O. and M.P. Fernandez, *Molecular phylogeny of annexins and identification of a primitive homologue in Giardia lamblia.* Mol Biol Evol, 1995. **12**(6): p. 967-79.
20. Almeida, P.F., *Annexin induces massive lipid demixing in bilayers modeling the plasma membrane inner leaflet.* Manuscript In Progress.
21. Brandts, J.F. and L.N. Lin, *Study of strong to ultratight protein interactions using differential scanning calorimetry.* Biochemistry, 1990. **29**(29): p. 6927-40.

22. Rosengarth, A., et al., *A comparison of the energetics of annexin I and annexin V.* J Mol Biol, 1999. **288**(5): p. 1013-25.
23. Kingsley, P.B. and G.W. Feigenson, *The synthesis of a perdeuterated phospholipid: 1,2 dimyristoyl-sn-glycero-3-phosphocholine-d72.* Chemistry and Physics of Lipids, 1979. **24**: p. 135-147.
24. Wiseman, T., et al., *Rapid measurement of binding constants and heats of binding using a new titration calorimeter.* Anal Biochem, 1989. **179**(1): p. 131-7.
25. Kenakin, T., *Allosteric theory: taking therapeutic advantage of the malleable nature of GPCRs.* Curr Neuropharmacol, 2007. **5**(3): p. 149-56.
26. Vaidehi, N. and T. Kenakin, *The role of conformational ensembles of seven transmembrane receptors in functional selectivity.* Curr Opin Pharmacol, 2010. **10**(6): p. 775-81.
27. Kenakin, T., *G-protein coupled receptors as allosteric machines.* Receptors Channels, 2004. **10**(2): p. 51-60.
28. Kenakin, T., *Functional selectivity and biased receptor signaling.* J Pharmacol Exp Ther, 2011. **336**(2): p. 296-302.
29. Monod, J., J. Wyman, and J.P. Changeux, *On the Nature of Allosteric Transitions: A Plausible Model.* J Mol Biol, 1965. **12**: p. 88-118.
30. Moravcevic, K., et al., *Kinase associated-1 domains drive MARK/PAR1 kinases to membrane targets by binding acidic phospholipids.* Cell, 2010. **143**(6): p. 966-77.
31. Draeger, A., K. Monastyrskaya, and E.B. Babiychuk, *Plasma membrane repair and cellular damage control: the annexin survival kit.* Biochem Pharmacol, 2011. **81**(6): p. 703-12.
32. Garcia-Saez, A.J., et al., *Membrane promotes tBID interaction with BCL(XL).* Nat Struct Mol Biol, 2009. **16**(11): p. 1178-85.
33. Takahashi, H., et al., *Interaction of synaptotagmin with lipid bilayers, analyzed by single-molecule force spectroscopy.* Biophys J, 2010. **99**(8): p. 2550-8.
34. Ferreon, A.C., et al., *Interplay of alpha-synuclein binding and conformational switching probed by single-molecule fluorescence.* Proc Natl Acad Sci U S A, 2009. **106**(14): p. 5645-50.
35. Almeida, P.F., *Thermodynamics of lipid interactions in complex bilayers.* Biochim Biophys Acta, 2009. **1788**(1): p. 72-85.
36. Fernández-Chacón, R., et al., *Synaptotagmin I functions as a calcium regulator of release probability.* Nature, 2001. **410**: p. 41-49.
37. Kochubey, O., X. Lou, and R. Schneggenburger, *Regulation of transmitter release by Ca(2+) and synaptotagmin: insights from a large CNS synapse.* Trends Neurosci, 2011. **34**(5): p. 237-46.
38. Zhang, X., J. Rizo, and T.C. Südhof, *Mechanism of phospholipid binding by the C2A-domain of synaptotagmin I.* Biochemistry, 1998. **37**: p. 12385-12403.
39. Shao, X., et al., *Solution structures of the Ca2+-free and Ca2+-bound C2A domain of synaptotagmin I: does Ca2+ induce a conformational change?* Biochemistry, 1998. **37**(46): p. 16106-15.
40. Xue, M., et al., *Structural and mutational analysis of functional differentiation between synaptotagmins-1 and -7.* PLoS One, 2010. **5**(9).
41. Smith, E.A. and J.C. Weisshaar, *Docking, not fusion, as the rate-limiting step in a SNARE-driven vesicle fusion assay.* Biophys J, 2011. **100**(9): p. 2141-50.
42. Christensen, S.M., M.W. Mortensen, and D.G. Stamou, *Single vesicle assaying of SNARE-synaptotagmin-driven fusion reveals fast and slow modes of both*

docking and fusion and intrasample heterogeneity. Biophys J, 2011. **100**(4): p. 957-67.
43. Luque, I., S.A. Leavitt, and E. Freire, *The linkage between protein folding and functional cooperativity: two sides of the same coin? .* Annu Rev Biophys Biomol Struct, 2002. **31**: p. 235-256.
44. Hilser, V.J. and E.B. Thompson, *Intrinsic disorder as a mechanism to optomize allosteric coupling in proteins.* Proc Natl Acad Sci USA, 2007. **104**: p. 8311-8314.
45. Santoro, M.M. and D.W. Bolen, *Unfolding free energy changes determined by the linear extrapolation method. 1. Unfolding of phylmethanesulfonyl α-chymotrypson using different denaturants.* Biochemistry, 1988. **27**: p. 8063-8068.
46. Streicher, W.W. and G.I. Makhatadze, *Unfolding thermodynamics of Trp-cage, a 20 residue miniprotein, studied by differential scanning calorimetry and circular dichroism spectroscopy.* Biochemistry, 2007. **46**(10): p. 2876-80.
47. De Levie, R., *Estimating Parameter Precision in Nonlinear Least Squares with Excel's Solver.* J Chem Educ, 1999. **76**: p. 1594-1598.
48. Spolar, R. S., J. R. Livingstone, and M. T. Record. 1992. Use of Liquid Hydrocarbon and Amide Transfer Data To Estimate Contributions to Thermodynamic Functions of Protein Folding from the Removal of Nonpolar and Polar Surface from Water. *Biochemistry.* 31:3947-3955.
49. Kumar, S., C.J. Tsai, and R. Nussinov, *Maximal stabilities of reversible two-state proteins.* Biochemistry, 2002. **41**(17): p. 5359-74.